Acc. Chem. Res. **2000,** *33,* 483−490

The Whole Story of the Two-Electron Bond, with the δ Bond as a Paradigm

F. ALBERT COTTON*,† AND
DANIEL G. NOCERA*,‡

Laboratory for Molecular Structure and Bonding and the Department of Chemistry, Texas A&M University, College Station, Texas 77843-3255, and Department of Chemistry, 6-335, Massachusetts Institute of Technology, Cambridge, Massachusetts 02139-4307

Received July 1, 1999

ABSTRACT

It is shown that the δ bond, as found particularly in the Re_2^{6+} and Mo_2^{4+} cores of hundreds of compounds, provides a paradigm for the behavior of two-electron bonds of all types. By control of the angle of twist around the M−M axis, the strength of the bond can be systematically varied. By means of conventional electronic spectroscopy, nuclear magnetic resonance spectroscopy, and two-photon excitation spectroscopy, the entire picture of the manifold of four states for two electrons bonding two atoms, as first described by Coulson and Fischer in 1949, has been confirmed.

"*The chemical bond is not so simple as some people seem to think.*" — R. S. Mulliken[1]

Introduction

It can be said without fear of contradiction that the two-electron bond is the single most important stereoelectronic feature of chemistry. This does not exclude multiple bonds since they are commonly, if not exactly rigorously, regarded as composed of two, three, or four, two-electron components.

The concept of a two-electron bond was first introduced by G. N. Lewis in 1916.[2] It was not possible at the time to describe it in any more detail than he did, namely, that a single bond is formed by a pair of shared electrons. Nor was it possible to represent it in any more detail than as a pair of dots placed between the symbols for two atoms, much as a line had been (and still is) used for the same purpose:

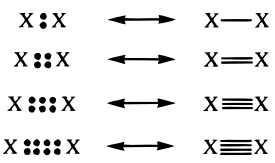

These simple representations of bonds are all a chemist needs in much of the usual discussion of chemical formulas, reactions, and other phenomena. Moreover, when the explicit recognition that "—" means ":" is coupled with the octet concept, a significant improvement occurs because this leads to better appreciation of the dependence of charge distribution (at least formally) and stereochemistry on electronic structure.[3]

With the advent of quantum mechanics, theoreticians acquired the tools to explore the nature of the two-electron bond in a much more profound way. From the start, the bond in the hydrogen molecule was taken as prototypical, for example by Heitler and London (1927) in their development of valence bond theory.[4] In 1933, James and Coolidge very laboriously showed[5] that a quantum mechanical calculation, when carried to a sufficient level of accuracy via the variation principle, could provide very accurate values for the length and energy of this bond. This validated both Lewis's proposal and the correctness of the quantum theory of chemical bonding.

Given that the application of the wave equation to the electronic structures of molecules was feasible and desirable, the question of how best to construct the appropriate wave functions came to the fore. A proposal made by Linus Pauling in 1928[6] and again by Lennard-Jones in 1929[7] gained support. This proposal was to construct orbitals for an entire molecule as superpositions of orbitals on the individual atoms. The method, which is now known as the LCAO (linear combination of atomic orbitals) approach, was first fully implemented in 1949 by Coulson and Fischer for the H_2 molecule.[8]

The work of Coulson and Fischer was seminal because it dealt with the bonding problem in all its aspects:

(1) It described the entire manifold of four electronic states that arises when there are two atoms, two orbitals, and two electrons.

(2) It described the electronic structure over the entire range of internuclear distances, from those shorter than the equilibrium distance for the ground state to the dissociation limit.

(3) It explicitly included, and drew attention to, the important role played by configuration interaction, i.e., the interaction of states of the same symmetry derived from different electron configurations.

In short, Coulson and Fischer gave us a complete picture of the two-electron bond as obtained by the LCAO−MO method of constructing wave functions. The results of

F. Albert Cotton is Distinguished Doherty-Welch Professor of Chemistry at Texas A&M University. He received his Ph.D. in 1955 from Harvard University and then spent 17 years at MIT before moving to Texas A&M in 1972. His laboratory reported the first examples of nearly all metal−metal multiple bonds, first formulated a quadruple bond ($Re_2Cl_8^{2-}$) in 1964, and has recently provided the first examples of an Nb^{II}−Nb^{II} triple bond, an Ir^{III}−Ir^{III} double bond, a Pd^{III}−Pd^{III} single bond, and the first $(Ti^{II})_3$ cluster compound.

Daniel G. Nocera is a Professor of Chemistry at the Massachusetts Institute of Technology. After performing graduate work at the California Institute of Technology (Ph.D., 1984) in the laboratories of Harry B. Gray, he moved to Michigan State University. There, he was on the faculty for 13 years before moving to MIT in 1997. He studies the basic mechanisms of energy conversion in biology and chemistry. He also invents new optical diagnostic techniques for the study of a variety of fluid physics and engineering problems.

† Texas A&M University.
‡ Massachusetts Institute of Technology.

10.1021/ar980116o CCC: $19.00
Published on Web 04/22/2000

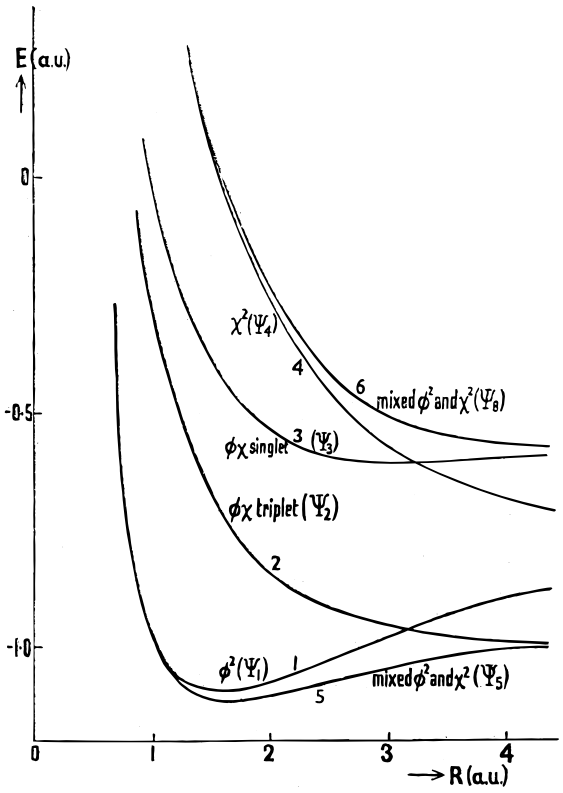

FIGURE 1. Energies of electronic states of the H_2 molecule vs internuclear distance, as published by Coulson and Fischer in 1949. Reprinted with permission from ref 8.

their treatment are represented in Figure 1, which is taken from their paper.

There is no reason to suspect that these results might be in any way incorrect, so long as it is agreed that wave mechanics itself, at this level of approximation at least, is correct. So what else is left to say? Perhaps *only* this: it is central to the concept of *scientific* research that all theoretical results, however little reason there might be to doubt their correctness, ought to be tested experimentally. Another way to put this is the following: to be fully scientific we should not only answer theoretical questions but question theoretical answers. But has the picture in Figure 1 ever been *fully* checked experimentally, namely, by showing experimentally how all four states behave as a function of bond strength (which is, in turn, determined by internuclear distance)? Clearly not, because except for a few aspects, this overall picture cannot be evaluated experimentally for the H−H σ bond, nor for any other σ bond. We cannot examine the evolution of all four states as we gradually and systematically stretch the molecule. Molecular tweezers are yet to be invented.

Here is where the δ bond enters the arena. The δ bond has the useful property that there are *two* ways to reduce its strength: (1) as for any bond, by increasing the internuclear distance, and (2) by changing the internal angle, χ, as defined in Figure 2, from 0° where the $\delta-\delta$ overlap is maximal, to 45° where the overlap becomes zero and the δ bond is abolished. It may not be immediately obvious why the δ bond should necessarily offer any advantage over a σ bond because the aforementioned lack

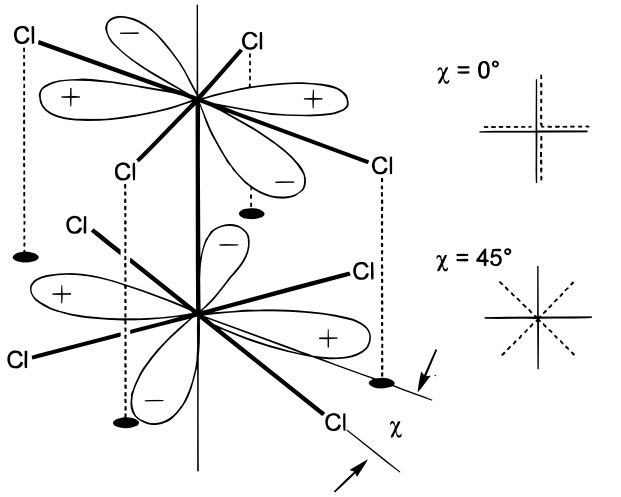

FIGURE 2. Diagrammatic representation of a δ bond and how the d_{xy}/d_{xy} overlap varies with the internal twist angle, χ.

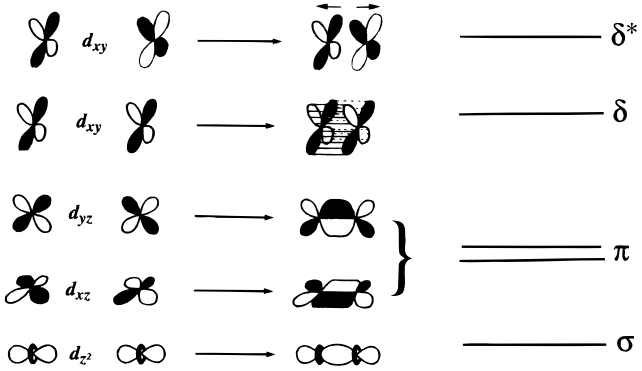

FIGURE 3. Diagram of the orbitals involved in forming a quadruple bond.

of molecular tweezers would appear to imply that we can no more twist a molecule at will than we can stretch it at will. But, by chemical means, we can, as will now be explained.

A Brief Chemical Background

Some background concerning the chemistry of compounds that contain a δ bond will first be necessary before we describe the work that has been done using the δ bond. While there was earlier mention of δ bonding, the concept became an indisputable reality only with the first report[9] of the quadruple bond in $Re_2Cl_8^{2-}$, which was soon followed by reports of quadruple bonds in other species.[10]

The quadruple bond consists of a σ bond, two equivalent π bonds, and the δ bond. A simplified energy level diagram is shown in Figure 3. Several important points that underlie the main theme can be made by referring to this diagram. First, the σ and two π bonds account for nearly all of the bonding between the metal atoms. This means that even with the loss of all the δ bonding (as in the case where one δ electron is promoted to the δ^* orbital), the bond length changes little (typically 3%).[11] Second, the bonding that arises from the $\sigma^2\pi^4$ configuration is independent of the internal twist angle. This means that a quadruply bonded M_2 unit together with the σ and

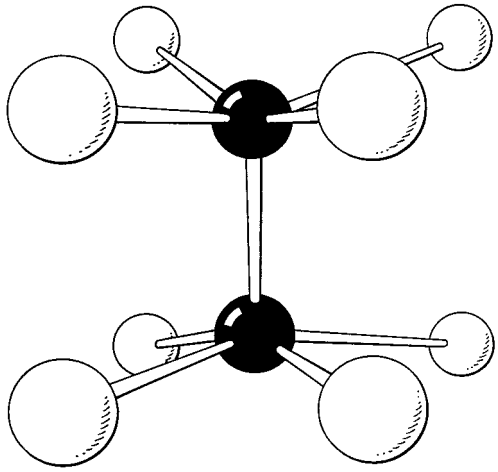

FIGURE 4. $M_2Cl_8^{n-}$ ions, with M = Re, $n = 2$ and M = Mo, $n = 4$.

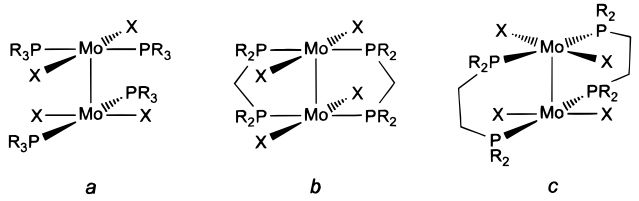

FIGURE 5. Three types of structures arising when four Cl^- ions are substituted by four PR_3 or two diphosphines.

π bonding therein is an (almost) fixed frame within which the dependence of δ bonding on the twist angle can be examined.

The earliest argument presented for the existence of a δ bond in $Re_2Cl_8^{2-}$ and the isoelectronic $Mo_2Cl_8^{4-}$ was based on the eclipsed rotational conformation of these ions[12] (Figure 4). The chemistry of the $Mo_2Cl_8^{4-}$ ion underwent a major development when it was found[13] that reaction 1 occurs, and that a similar sort of reaction 2 occurs[14] with diphosphines, $R_2P(CH_2)_nPR_2$ (P−P). Continued investigation of these complexes included extensive structural and spectroscopic studies.[15]

$$Mo_2Cl_8^{4-} + 4PR_3 \rightarrow Mo_2Cl_4(PR_3)_4 + 4Cl^- \qquad (1)$$

$$Mo_2Cl_8^{4-} + 2P{-}P \rightarrow Mo_2Cl_4(P{-}P)_2 + 4Cl^- \qquad (2)$$

As shown in Figure 5, the main structural results were that (a) the $Mo_2X_4(PR_3)_4$ species always had a structure of type **a**, in which the internal torsion (twist) angle is zero, (b) the $Mo_2X_4(R_2PCH_2PR_2)_2$ molecules always have a structure of type **b**, wherein the twist angle is again zero, and (c) compounds of the type $Mo_2X_4(R_2P(CH_2)_nPR_2)$ ($n = 2$, 3, or 4) have a structure of type **c** but with a range of twist angles, depending on the identities of R and X and the number of methylene subunits in the ligand backbone. In some molecules of type **c** the P−Mo−Mo−P torsion angle exceeds 45°. In view of the symmetry of the δ orbitals, however, χ angles 0−45° and 45−90° are equivalent insofar as the d_{xy}/d_{xy} overlap is concerned.

The most important result of these studies in the present context was that there is a relationship between the twist angle and the energy of the $\delta \rightarrow \delta^*$ absorption band,[16] as shown in Figure 6. We see here that the extrapolated $\delta-\delta^*$ transition energy at $\chi = 45°$ ($\cos 2\chi = 1$) is not zero even though the $\delta-\delta$ overlap is zero. How can this be? Because, as already shown by Coulson and Fischer for a stretched H_2 molecule, the energies of the four electronic states that exist for the molecule in its normal bonded state converge, pairwise, to two energies, and these are separated by an energy $2K$, where K is a quantity in electronic structure theory called the exchange energy. What the data in Figure 6 enable us to do is to measure, approximately, but *directly from experiment*, the value of K for a chemical bond. This had never been done before. Even more interesting was the idea that by making further measurements on actual molecules that have twist angles between 0° and 45°, it might be possible to trace the behavior of all four states of the δ bond manifold as a function of $\delta-\delta$ overlap and see if they follow the pattern implied by the work of Coulson and Fischer for any two-electron bond.

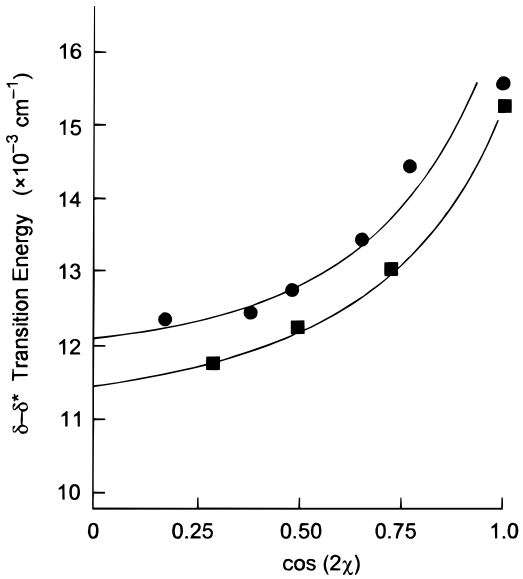

FIGURE 6. Energies of the $^1(\delta\delta \rightarrow \delta\delta^*)$ transition for a series of $Mo_2X_4L_4$ and $Mo_2X_4(P{-}P)_2$ compounds, where L and P−P are mono- and diphosphine ligands, plotted against the internal twist angle χ. The upper curve is for compounds in which X = Cl and the lower one for X = Br. (Taken from ref 16).

A Brief Theoretical Background

Before explaining what has been done experimentally, we shall briefly review the LCAO method as it applies to *any* two-electron bond. It is important to do this because what might be done for a δ bond is, mutatis mutandis, applicable to σ bonds and π bonds as well. [Note: In principle, π bonds can also be weakened by twisting as well as by stretching, but they do not lend themselves as well as δ bonds to full-range characterization because, to abolish a π bond, a 90° twist is required. In fact, the largest twist that has been reported for a ground-state structure is only 40° (Leuf, W.; Reese, R. *Top. Stereochem.* **1991**, *20*, 231), and because π bond strength varies as $\cos \chi$, a 40° twist covers less than a quarter of the total π bond strength range.]

For any two-center, homonuclear bond, whether σ, π, or δ, an LCAO−MO treatment begins with the following four steps:

(1) Let the atomic orbitals on atoms 1 and 2 be designated γ_1 and γ_2.

(2) The bonding, ϕ, and antibonding, χ, LCAO−MOs (neglecting overlap) are

$$\phi = \frac{1}{\sqrt{2}}(\gamma_1 + \gamma_2)$$

$$\chi = \frac{1}{\sqrt{2}}(\gamma_1 - \gamma_2)$$

(3) The energies of these MOs are

$$E_\phi = \langle\phi|H|\phi\rangle$$
$$= \int \gamma_i H \gamma_i \, d\tau + \int \gamma_1 H \gamma_2 \, d\tau \quad \text{where } i = 1 \text{ or } 2$$
$$= E_\gamma + W \quad (W < 0)$$
$$E_\chi = E_\gamma - W$$

Since E_γ is the energy of one electron in the atomic orbital γ_1 or γ_2, we may take this as the zero of energy and write

$$E_\phi = W \qquad \text{and} \qquad E_\chi = -W$$

If there is only one electron to occupy these MOs, we have a very simple (and very familiar) picture, as shown in Figure 7. There are only two *states*, ϕ and χ, and only one electronic transition, namely, that from the ground state to the excited state, whose energy is exactly $2W$. But what happens when there are two electrons?

(4) We must now write determinantal wave functions for the four states that can arise. If both electrons occupy the ϕ MO, to give a full bond, we have

$$\Psi_1 = \left|\phi^{+}\bar{\phi}\right| = \frac{1}{\sqrt{2}}\begin{vmatrix}\phi^{+}(1) & \bar{\phi}(1)\\ \phi^{+}(2) & \bar{\phi}(2)\end{vmatrix}$$

$$= \frac{1}{\sqrt{2}}\left[\phi^{+}(1)\bar{\phi}(2) - \bar{\phi}(1)\phi^{+}(2)\right]$$

After separating orbital and spin functions, using α ($= {}^1/_2$) and β ($= -{}^1/_2$) for the latter, we obtain

$$\psi_1 = \frac{1}{\sqrt{2}}\phi(1)\phi(2)[\alpha\beta - \beta\alpha]$$

where the antisymmetrization required by the Pauli principle is accomplished by the spin function. We could also place both electrons in the χ MO and get an analogous expression,

$$\psi_1 = \frac{1}{\sqrt{2}}\chi(1)\chi(2)[\alpha\beta - \beta\alpha]$$

Both of these represent spin singlet states.

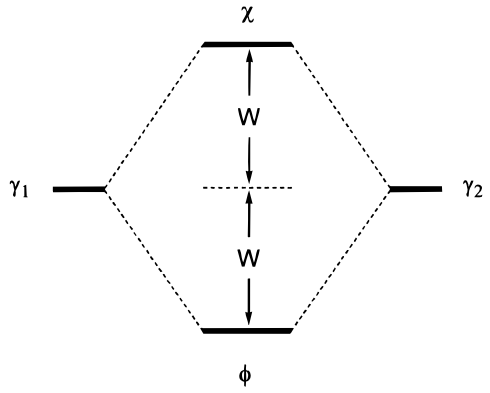

FIGURE 7. Energy level diagram for a δ bond (or other bond) when only one δ electron is present.

Because the Pauli principle no longer restricts us to antisymmetrizing the wave function by way of the spins, we have two possibilities when we develop the corresponding expressions for the states arising from placing one electron in ϕ and the other in χ. Spin-paired electrons give a singlet state, but antisymmetrization can also be done if both electrons have the same spin by way of an antisymmetric orbital (i.e., spatial) function, giving a triplet state. Altogether, we have the following four states in what is called the bond manifold:

$$\psi_1 = \frac{1}{\sqrt{2}}\phi(1)\phi(2)[\alpha\beta - \beta\alpha]$$

$$\psi_2 = \frac{1}{\sqrt{2}}[\phi(1)\chi(2) - \phi(2)\chi(1)]\begin{cases}[\alpha\alpha]\\ \frac{1}{\sqrt{2}}[\alpha\beta + \beta\alpha]\\ [\beta\beta]\end{cases}$$

$$\psi_3 = \frac{1}{2}[\phi(1)\chi(2) + \phi(2)\chi(1)][\alpha\beta - \beta\alpha]$$

$$\psi_4 = \frac{1}{\sqrt{2}}\chi(1)\chi(2)[\alpha\beta - \beta\alpha]$$

The two-term orbital factors in ψ_2 and ψ_3 arise because of the indistinguishability of electrons; we cannot assert that electron 1 is in ϕ and electron 2 in χ rather than the reverse, so we must give both assignments equal weight.

These four steps set up our problem. We now have to determine the energies of the four states. Before actually doing so, we pause to note that most chemists would "intuitively" (whatever that means exactly) expect the following order of increasing energy,

$$\psi_1 \ll \psi_2 \approx \psi_3 \ll \psi_4$$

on the grounds that ψ_1 represents a net bond, ψ_2 and ψ_3 involve the promotion of one electron and represent no net bond, and ψ_4 involves a two-electron promotion and is completely antibonding.

This, however, is not the case; to find out why, we must first derive expressions for the state energies and also look more closely at the wave functions. There are several computational approaches that can be used, including a generalized valence bond (GVB) method.[17] Since this is, perhaps, not as transparent to most chemists as the

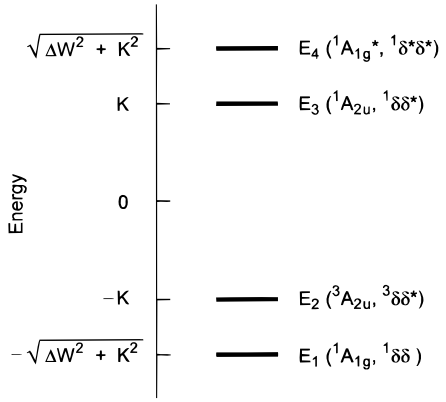

FIGURE 8. Energy level diagram for the states of the δ manifold when two electrons are present. $\Delta W = E_\chi - E_\phi$.

LCAO−MO method, we shall continue to develop our arguments by the latter method. We shall, however, return to the valence bond approach later.

For E_1 and E_4 we must obtain the roots of a quadratic equation, because ψ_1 and ψ_4 have the same symmetry and the true wave functions for the highest and lowest states of the manifold are not ψ_1 and ψ_4 but, as we shall see in detail shortly, mixtures of both. For E_2 and E_3 we have simple, independent expressions. The entire set of results is

$$\begin{vmatrix} 2W + J_{\phi\phi} - E & K \\ K & -2W + J_{\chi\chi} - E \end{vmatrix} = 0$$

$$\text{where } E_- = E_1 \text{ and } E_+ = E_4$$

$$E_2 = J_{\phi\chi} - K$$

$$E_3 = J_{\phi\chi} + K$$

In these equations, $\pm W$ has the same meaning as before, namely, it is the energy by which ϕ or χ, as a one-electron orbital, is lowered or raised, respectively, from their average value. $J_{\phi\phi}$, $J_{\chi\chi}$, and $J_{\phi\chi}$ are Coulomb integrals, inherently positive, and represent the repulsive interaction between the charge clouds of two electrons that are either in the same orbital ($J_{\phi\phi}$, $J_{\chi\chi}$) or in different orbitals ($J_{\phi\chi}$). Finally we have K, the exchange integral, which is simply half the energy required, for two atoms, X, infinitely far apart, to convert $X^\bullet + X^\bullet$ to $X^+ + X^-$.

Everything said so far applies to any type of two-electron bond. However, it is best now to focus more directly on the particular case of the δ bond as it occurs in a species such as $Mo_2Cl_8^{4-}$, where the symmetry is D_{4h}. Accordingly, we shall henceforth assign to the four states of the δ manifold their appropriate symmetries, i.e., $^1A_{1g}$, $^3A_{2u}$, $^1A_{2u}$, and $^1A_{1g}$* for $^1\delta\delta$, $^3\delta\delta^*$, $^1\delta\delta^*$, and $^1\delta^*\delta^*$, respectively. For convenience of presentation, we will preserve this D_{4h} state parentage description in our later discussion of the lower symmetry molecules of Figure 5.

Simple though they are, the energy equations are still a bit awkward. Therefore, as suggested by Hopkins, Gray, and Miskowski,[18] since the overlap between two δ type d orbitals is always small, one may assume $J_{\phi\phi} = J_{\chi\chi} \approx J_{\phi\chi}$. This, then, allows us to omit the J's altogether since they change each energy additively in the same direction. We can now draw the energy level diagram shown in Figure 8. It will be noted that here the relative energies of the four states follow the pattern $E_1 < E_2 \ll E_3 < E_4$, rather than the "intuitive" pattern mentioned earlier. This happens because $2K \gg W$ for δ bonds as a result of the weak overlap resulting from the parallel disposition of the d_{xy} orbitals. For example, in $Mo_2Cl_8^{4-}$, $2K/W \approx 4$.

Let us now return to the wave functions previously written for the four states and see what they tell us about the electron distribution in each state. If we take the state wave functions and substitute in the LCAO expressions for ϕ and χ, we obtain the following results:

	Ionic		Covalent
ψ_1 =	$[\gamma_1(1)\gamma_1(2) + \gamma_2(1)\gamma_2(2)]$	+	$[\gamma_1(1)\gamma_2(2) + \gamma_2(1)\gamma_1(2)]$
ψ_2 =			$[\gamma_1(1)\gamma_2(2) + \gamma_2(1)\gamma_1(2)]$
ψ_3 =	$[\gamma_1(1)\gamma_1(2) + \gamma_2(1)\gamma_2(2)]$		
ψ_4 =	$[\gamma_1(1)\gamma_1(2) + \gamma_2(1)\gamma_2(2)]$	−	$[\gamma_1(1)\gamma_2(2) + \gamma_2(1)\gamma_1(2)]$

States 1−4 here correspond to those numbered 1, 2, 3, and 4 in Figure 1. We see that ψ_2 and ψ_3 which are the actual wave functions (so long as we treat the δ manifold alone) are, respectively, purely covalent and purely ionic. On the other hand, ψ_1 and ψ_4 both have half covalent and half ionic character. These are not credible wave functions as they stand. It is not, for example, believable that in the $^1A_{1g}$ state there are two electrons on one atom half the time. The ionic distribution must be of much higher energy than the covalent one and, accordingly, should contribute mainly to the $^1A_{1g}$* state, while the $^1A_{1g}$ ground state should be mainly covalent. This is, in fact, exactly what occurs. The wave functions ψ_1 and ψ_4 are not really the orbital wave functions for the $^1A_{1g}$ and $^1A_{1g}$* states; through the off-diagonal element, these two orbital wave functions are mixed (configuration interaction) and the true orbital wave functions for these two states are given by

$$\psi(^1A_{1g}) = \psi_1 - \lambda\psi_4$$

$$\psi(^1A_{1g}^*) = \psi_4 + \lambda\psi_1$$

If we examine the expressions for ψ_1 and ψ_4 given above we see that as λ increases, $\psi(^1A_{1g})$ becomes more covalent and $\psi(^1A_{1g}^*)$ becomes more ionic. This mixing contributes to the stability of the $^1A_{1g}$ ground state and raises the energy of the $^1A_{1g}$* state.

Energy Measurements of the δ Bond Manifold

We can show the essence of what has just been done in a very simple diagram of the four states, and how their energies would be expected to evolve as the $\delta-\delta$ interaction proceeds from its maximum when the molecule is eclipsed ($\chi = 0°$, $\cos 2\chi = 1$) through intermediate angles to the situation in the perfectly staggered molecule ($\chi = 45°$, $\cos 2\chi = 0$). Such a diagram is presented in Figure

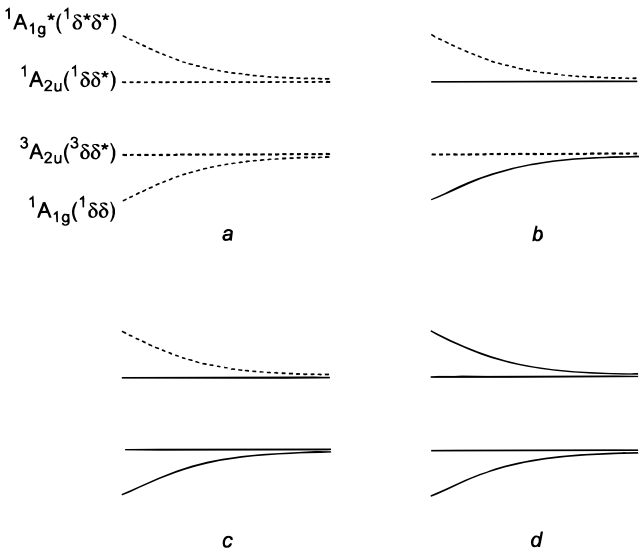

FIGURE 9. Diagrams showing qualitatively how the work progressed from a wholly theoretical basis (a), through the intermediate stages (b) and (c), to a completely experimental basis (d).

9a, where the four states are represented by broken lines, meant to represent everything that was, initially, predicted but not yet experimentally verified. This diagram is basically the same as what is shown in Figure 1 by the curves 2, 3, 5, and 6, which are the Coulson and Fischer results that take account of configuration interaction.

If we now refer back to the experimental results presented in Figure 6, it is easily seen that they can be used to transform Figure 9a to Figure 9b. That is, we can change two of the theoretical lines (broken) to experimental lines (solid). The $^1A_{1g} \rightarrow {}^1A_{2u}$ transition, commonly referred to simply as the $\delta \rightarrow \delta^*$ transition, does indeed start at a high value, 15 000−16 000 cm^{-1} at $\chi = 0$ and asymptotically approach a much lower value, ca. 12 000 cm^{-1}, as $\chi \rightarrow 45°$. The question remaining is, "How much further can we go in demonstrating experimentally that the *entire* picture in Figure 9a is correct?"

To convert *all* of the theoretical picture to experimental fact, it is necessary to measure two more independent energy separations. There are four choices: $^1A_{1g}-{}^3A_{2u}$, $^1A_{1g}-{}^1A_{1g}{}^*$, $^3A_{2u}-{}^1A_{2u}$, and $^3A_{2u}-{}^1A_{1g}{}^*$. At first sight, none of these measurements appears easily feasible, but the last two look really hopeless. The difficulty with each of the first two is that the corresponding spectroscopic transitions are forbidden. The first is spin-forbidden and the second is forbidden because it is a two-electron transition. When the spin-forbiddeness of the $^1A_{1g} \rightarrow {}^3A_{2u}$ transition is added to the fact that even the spin-allowed $^1A_{1g} \rightarrow {}^1A_{2u}$ transition is weak, one cannot be too surprised that it has never been observed directly in any molecule. However, both of these forbiddeness problems have been overcome.

The first problem that was solved was the measurement of the $^1A_{1g}-{}^3A_{2u}$ energy difference. The method employed depends on the fact that the $^1A_{1g}-{}^3A_{2u}$ energy gap is small, especially as the bond is twisted and the $\delta-\delta$ overlap is lessened. When the torsion angle is in the range of 20−40° (or, equivalently, 50−70°), the gap is of the order of kT at and below room temperature. Therefore, there is enough thermal population of the $^3A_{2u}$ state, following a Boltzmann distribution, to cause a measurable change in the chemical shift of the ^{31}P resonance, without making the line too broad for accurate measurement. This NMR method was used[19] for several of the $Mo_2Cl_4(P-P)_2$ compounds to afford $^1A_{1g}-{}^3A_{2u}$ energy gaps for six compounds of the $Mo_2Cl_4(P-P)_2$ type, with χ values of 24.7°, 41.4°, 50.0°, 59.5°, 64.5°, and 69.4°. These data define a line that is parallel, within experimental error, to the line for the $^1A_{2u}$ state. The $^1A_{2u}-{}^3A_{2u}$ separations are in the range 10 190−10 780 cm^{-1}, average 10 440 ± 180 cm^{-1}. Thus, we can add another solid line to Figure 9b so as to obtain Figure 9c.

We now have the problem of getting from Figure 9c to Figure 9d, that is, relating the energy of the $^1A_{1g}{}^*$ state to the energies of the other three states by experimental measurements. That task was addressed in the following way. We first observe that, although forbidden by one-photon selection rules, the $^1A_{1g} \rightarrow {}^1A_{1g}{}^*$ transition is allowed in the two-photon absorption spectrum. Here, two δ electrons are promoted to the δ^* level by the simultaneous absorption of two photons whose energies sum to the energy required for the transition. Because we can estimate the $^1A_{1g} \rightarrow {}^1A_{1g}{}^*$ transition energy from our knowledge of $^1A_{1g} \rightarrow {}^1A_{2u}$, we recognize that the two exciting photons must be in the near-infrared frequency range. Moreover, the simultaneous absorption of two photons is an unlikely event, the probability of which increases with the square of the intensity of the absorbing light, so the flux of the exciting photons must be intense. These demanding conditions of intense and tunable near-infrared photons can be satisfied with the output from optical parametric oscillators. But providing the necessary laser excitation source constitutes only one half of the experimental problem. There is also the question of how one knows when $^1A_{1g} \rightarrow {}^1A_{1g}{}^*$ is occurring? The most obvious approach would be to measure the transmittance, but this is impractical for a two-photon experiment and especially so when the spin-allowed transitions are weak, as is the case within the δ manifold.

A more promising strategy is to monitor a fluorescence intensity that is dependent on the population of the $^1A_{1g}{}^*$ state. Although $^1A_{1g}{}^*$ is sure to be photon-silent, its neighboring $^1A_{2u}$ excited state may be emissive for selected quadruple bond metal complexes. Because the $^1A_{1g}{}^* \rightarrow {}^1A_{2u}$ conversion is fully allowed, $^1A_{1g}{}^*$ may internally convert to $^1A_{2u}$ on a much faster time scale than that associated with emissive decay from the $^1A_{2u}$ state. Therefore, as the two-photon laser excitation frequency is tuned into the $^1A_{1g}{}^*$ excited state, emission from $^1A_{2u}$ can be observed. Conversely, no $^1A_{2u}$-based luminescence will be generated when the two near-infrared photons are off resonance from the $^1A_{1g} \rightarrow {}^1A_{1g}{}^*$ transition. In this manner, the absorption profile of the $^1A_{1g}{}^*$ state can be mapped out (at twice the excitation frequency) by monitoring the laser-induced fluorescence (LIF) from the $^1A_{2u}$ excited state as the near-infrared spectral region is scanned.

On the basis of these considerations, the first experiment undertaken employed the LIF technique in a case

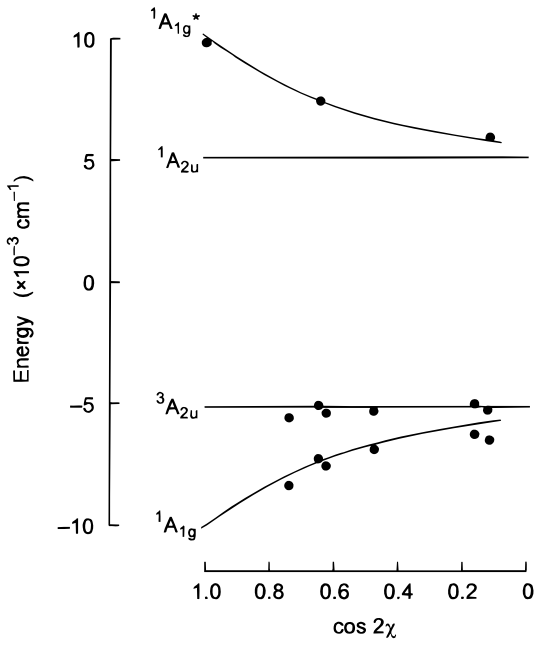

FIGURE 10. Actual experimental state energies vs cos 2χ for the $Mo_2X_4(P-P)_2$ molecules. Data from refs 16, 19, 20, and 22.

where $\chi = 0°$.[20] A complex of the type shown in Figure 5a was chosen, with R = Me, because it was already known that a prompt and strong $^1A_{2u} \rightarrow {}^1A_{1g}$ emission occurs.[21] The reason for this is that steric factors lock in the geometry so that, even though the δ bond is abolished in the $^1A_{2u}$ state, the two states have essentially the same structure. By monitoring the two-photon LIF from $Mo_2Cl_4(PMe_3)_4$, the $^1A_{1g}$* excited state was found to lie 4800 cm^{-1} above the $^1A_{2u}$ excited state. It will be noted immediately that this result agrees well with the energy gap expected from the $^1A_{1g}-{}^3A_{2u}$ curves of Figure 10 at $\chi = 0$.

Measurements of the $^1A_{1g}-{}^1A_{1g}$* energy gaps for complexes rotated away from an eclipsed ligand geometry are necessary to track the behavior of the $^1A_{1g}$* state across the diagram. However, such measurements pose a greater challenge to the two-photon LIF technique for two reasons. First, because many $Mo_2Cl_4(P-P)_2$ complexes do not emit, the number of complexes that can be investigated is limited. Second, as the twist angle is increased, the $^1A_{1g} \rightarrow {}^1A_{2u}$ absorption shifts into the red spectral region and consequently the associated $^1A_{2u} \rightarrow {}^1A_{1g}$ luminescence should occur further into the near-infrared where the response function of conventional detectors is diminished. Fortunately, the two $Mo_2Cl_4(P-P)_2$ complexes with $\chi = 24.7°$ and 41.4° (P−P = $Ph_2P(CH_2)_4PPh_2$ and $Et_2P(CH_2)_2PEt_2$, respectively) emit at sufficiently high energy and with enough intensity that the $^1A_{2u}$ fluorescence can be captured with red-sensitive detectors.[22] The $^1A_{1g}-{}^1A_{1g}$* energy gap measurements of these two complexes are particularly pertinent to constructing the plot of Figure 10 because these energy differences are near the mid- and endpoints of the correlation. As can be seen from these data, the $^1A_{1g}-{}^1A_{1g}$* separation monotonically decreases with increasing χ.

As shown in Figure 10, the complete experimental results correspond very well to the anticipated picture, as shown in Figure 9d. Perfectly quantitative agreement could not be expected because certain small effects have been neglected. First, we might note that we have been treating the states of the δ manifold as though they are completely isolated from all other electronic states in the molecule. This is a reasonable but obviously imperfect approximation.[23] We have also ignored the possible differences between the two configurations with $\chi = 0°$, namely that with the PR_3 groups eclipsed and that in which they are staggered. Finally, we have not taken account of small vibrational energy differences. For instance, the NMR measurements of the $^1A_{1g}-{}^3A_{2u}$ energy gaps involve molecules that are thermally equibrated in each state and thus provide true 0,0 transitions. On the other hand, the method of measuring the $^1A_{1g}-{}^1A_{1g}$* gaps provides vertical transition energies, where the $^1A_{1g}$* molecules must be, to some extent, vibrationally excited.

Despite such caveats, of which we are well aware, a beautiful picture, *directly from experiment*, of the manifold of states as a function of bond strength for a two-electron bond has been obtained for the first time. As stated at the outset, the relationships inherent in the Coulson−Fischer treatment of the hydrogen molecule were not in any sense suspect, but for science to be science, theoretical predictions must be confirmed experimentally. What has now been accomplished is to find a situation in which the necessary experimental evidence is obtainable and to obtain it, in full.

We acknowledge generous support from the National Science Foundation in both our laboratories. We also thank Professor B. E. Bursten for a critical reading of the manuscript and many helpful suggestions.

References

(1) Cf.: Coulson, C. A. Present State of Molecular Structure Calculations. *Rev. Med. Phys.* **1960**, *32*, 177.
(2) Lewis, G. N. The Atom and the Molecule. *J. Am. Chem. Soc.* **1916**, *38*, 762.
(3) Burdett, J. K. *Molecular Shapes. Theoretical Models of Inorganic Stereochemistry*; John Wiley & Sons: New York, 1980.
(4) Heitler, W.; London, F. Wechselwirkung neutraler Atome und homöopolare Bindung nach der Quantenmechanik. *Z. Phys.* **1927**, *44*, 455.
(5) James, H. M.; Coolidge, A. S. The Ground State of the Hydrogen Molecule. *J. Chem. Phys.* **1933**, *1*, 825.
(6) Pauling, L. The Application of the Quantum Mechanics to the Structure of the Hydrogen Molecule and the Hydrogen Molecule-ion and to Related Problems. *Chem. Rev.* **1928**, *5*, 173-213.
(7) Cf.: Slater, J. C. *Solid State and Molecular Theory: A Scientific Biography*; John Wiley & Sons: New York, 1975.
(8) Coulson, C. A.; Fischer, I. Notes on the Molecular Orbital Treatment of the Hydrogen Atom. *Philos. Mag.* **1949**, *40*, 386.
(9) (a) Cotton, F. A.; Curtis, N. F.; Johnson, B. F. G.; Robinson, W. R. Compounds Containing Dirhenium(III) Octahalide Anions. *Inorg. Chem.* **1965**, *4*, 326. (b) Cotton, F. A.; Harris, C. B. The Crystal and Molecular Structure of Dipotassium Octachlorodirhenate(II) Dihydrate, $K_2[Re_2X_8]\cdot 2H_2O$. *Inorg. Chem.* **1965**, *4*, 330. (c) Cotton, F. A. Metal−Metal Bonding in $[Re_2X_8]^{2-}$ Ions and Other Metal Atom Clusters. *Inorg. Chem.* **1965**, *4*, 334.
(10) For an account of this period, see: Cotton, F. A.; Walton, R. A. *Multiple Bonds between Metal Atoms*, 2nd ed.; Clarendon Press: Oxford, 1993; Chapter 1.
(11) Campbell, F. L., III.; Cotton, F. A.; Powell, G. L. Steric and Electronic Factors Influencing the Structures of Bridged (β-Type) $M_2Cl_4(LL)_2$ (M = Mo, Re) Compounds: A Refined Correlation of Bond Length with Torsion Angle. *Inorg. Chem.* **1985**, *24*, 4384.
(12) Bennett, M. J.; Caulton, K. G.; Cotton, F. A. The Structure of Tetra-η-butyratodiruthenium Chloride, a Compound with a Strong Metal−Metal Bond. *Inorg. Chem.* **1969**, *8*, 1.

(13) San Filippo, J., Jr. Diamagnetic Anisotropy Induced by Metal−Metal Bonds. *Inorg. Chem.* **1972**, *11*, 3140.
(14) Best, S. A.; Smith, T. J.; Walton, R. A. Complex Halides of the Transition Metals. 24. Reactions of Dimeric Molybdenum(II) Halide Complexes Containing Strong Metal−Metal Bonds with Bidentate Tertiary Phosphines and Arsines. Evidence for the Staggered Configuration in Dimers of Molybdenum(II). *Inorg. Chem.* **1978**, *17*, 99.
(15) Cotton, F. A.; Walton, R. A. *Multiple Bonds between Metal Atoms*, 2nd ed.; Clarendon Press: Oxford, 1993.
(16) Campbell, F. L., III.; Cotton, F. A.; Powell, G. L. $\delta \rightarrow \delta^*$ Transition Energies as a Function of δ-Bond Strength: An Extrapolative Assessment of the Ground-State Electron Correlation Energy. *Inorg. Chem.* **1985**, *24*, 177.
(17) Hay, P. J. Electronic States of the Quadruply Bonded $Re_2Cl_8^{2-}$ Species: An Ab Initio Theoretical Study. *J. Am. Chem. Soc.* **1982**, *104*, 7007.
(18) Hopkins, M. D.; Gray, H. B.; Miskowski, V. M. $\delta-\delta^*$ Revisited: What the Energies and Intensities Mean. *Polyhedron* **1987**, *6*, 705.
(19) Cotton, F. A.; Eglin, J. L.; Hong, B.; James, C. A. Singlet−Triplet Separations Measured by $^{31}P\{^1H\}$ NMR: Applications to Quadruply Bonded Dimolybdenum and Ditungsten Complexes. *Inorg. Chem.* **1993**, *32*, 2104.
(20) Engebretson, D. S.; Zaleski, J. M.; Leroi, G. E.; Nocera, D. G. Direct Spectroscopic Detection of a Zwitterionic Excited State. *Science* **1994**, *265*, 759.
(21) Hopkins, M. D.; Gray, H. B. Nature of the Emissive Excited State of Quadruply Bonded $Mo_2X_4(PMe_3)_4$ Complexes. *J. Am. Chem. Soc.* **1984**, *106*, 2468.
(22) (a) Engebretson D. S.; Graj, E. M.; Leroi, G. E.; Nocera, D. G. Two Photon Excitation Spectrum of a Twisted Quadruple Bond Metal−Metal Complex. *J. Am. Chem. Soc.* **1999**, *121*, 868. (b) Engebretson, D. S.; Nocera, D. G., unpublished result for $Et_2PCH_2CH_2PEt_2$.
(23) Bursten, B. E.; Clayton, T. W., Jr. A Simplified View of $\delta-\delta^*$ Transition Energies in Compounds with Multiple Metal−Metal Bonds: The Isolated $\delta-\delta^*$ Manifold Model. *J. Cluster Sci.* **1994**, *5*, 157. This excellent article deals in greater detail with several points that have been treated heuristically here, including the question of what happens when $\chi = 45°$ (exactly).

AR980116O